Microsyst Technol (2015) 21:1173–1178
DOI 10.1007/s00542-014-2188-6

CrossMark

TECHNICAL PAPER

Design and investigation of a low insertion loss, broadband, enhanced self and hold down power RF-MEMS switch

Mahesh Angira · Kamaljit Rangra

Received: 28 February 2014 / Accepted: 15 April 2014 / Published online: 27 May 2014
© Springer-Verlag Berlin Heidelberg 2014

Abstract This paper presents a low insertion loss capacitive shunt RF-MEMS switch. In the presented design, float metal concept is utilized to reduce the capacitance in up-state of the device. Float metal switch shows an insertion loss <0.11 dB, a return loss below 26.27 dB up to 25 GHz as compared to 0.81 dB insertion, 8.67 dB return loss for the conventional switch without float metal. OFF state response is same for the both devices. Further pull-in voltage of 12.75 V and switching time of 69.62 μs have been observed in case of the conventional switch whereas device with float metal have 11.75 V and 56.41 μs. Improvement of around 2.5 times in bandwidth and 4 times in input power has been observed without self actuation, hold down problem. The designed switch can be useful at device and sub-system level for multi-band applications.

1 Introduction

Telecommunication industries are growing at a rapid pace. New wireless standards are coming-up requiring devices with high linearity, low power consumption, large bandwidth. RF-MEMS is becoming an attractive technology for the above cited purpose. Amongst the different device switches have gained much attention. RF-MEMS switches have many telecommunication applications including cellular based station, mobile handsets, tunable filters, phased array antenna, signal routing, phase shifters as these switches offer better isolation, low insertion loss and less power consumption over a wider range of frequency as compared to solid state switches (Brown 1998; Rebeiz 2003, 2001; Tilmans 2003; Rangra 2005; Rangra et al. 2005; Angira et al. 2013).

However, at the sub-system/system level performance requirement becomes more stringent e.g. in multi-port switches (DiNardo et al. 2006; Kang et al. 2009), tunable filters (Peroulis et al. 2000; Entesari and Rebeiz 2005; Guo and Jin 2011), phased array antenna (Armenta et al. 2012), phase shifters (Rebeiz et al. 2002; Dey and Koul 2012; Razeghi and Ganji 2013) and switch Matrix (Fomani and Mansour 2009). The less insertion loss and broadband nature now become more essential. In the same context, a float metal based capacitive shunt RF-MEMS switch has been designed and investigated in this paper.

In shunt capacitive switch, ON and OFF state can be achieved by changing the value of capacitance between the movable structure and the transmission line. Thus a figure of merit is the ratio of capacitance in the down to up-state position of the movable beam. However, degraded capacitance in the down-state due to surface micro-roughness decreases the capacitance ratio (Yua et al. 2005, 2006). This makes the down-state behavior unpredictable in terms of resonant frequency. Float metal presents a good solution for the above cited problem. This concept also allows to reduce the RF overlap area between the movable structure and central conductor of CPW without affecting the down-state response and thus improves the insertion loss of the device (Giacomozzi et al. 2008).

In the presented work, float metal shunt capacitive switch has been compared to the conventional approach in terms of pull-in voltage, switching time, insertion loss,

M. Angira (✉)
Department of Electrical and Electronics Engineering, Birla Institute of Technology and Science, Pilani 333031, Rajasthan, India
e-mail: m.angira@gmail.com

K. Rangra
Central Electronics Engineering Research Institute, Pilani, Rajasthan, India

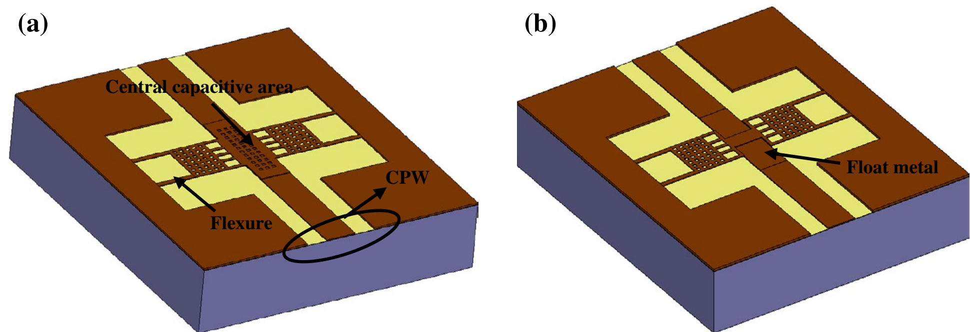

Fig. 1 Shunt capacitive switch (**a**) conventional (**b**) float metal

Table 1 Dimensions of the designed switches

Dimensions	Value
Length of bridge flexures	115 µm
Width of bridge flexures	15 µm
Thickness of all flexures	2 µm
Silicon dioxide thickness (t_{ox})	0.1 µm
Float metal thickness	0.2 µm
Electrostatic Gap (g_o)	2.7 µm
RF gap (d_o)	2.0 µm
Electrostatic actuation area ($A_{electro}$)	300 × 110 µm^2
RF central overlap (A_{float_RF}, A_{con_RF})	90 × 50 µm^2, 310 × 90 µm^2

isolation, bandwidth and power handling capability. For actuation, electrostatic method is used because of its compatibility with IC technology. The Switch is implemented as a broadside placed bridge structure. A uniform bridge structure requires higher pull-in voltage so four flexures attached to a central plate have been chosen to reduce the pull-in voltage. Figure 1a, b shows the model of the designed switches.

2 Device description and working

As typical of shunt configuration the input and output RF ports are physically connected to each other and therefore normally switch is ON. Broadside switch is based on a 50 Ω CPW line with 55/90/55 µm. The switches have a central overlap area of 310 × 90 µm^2, 90 × 50 µm^2 in conventional and float metal design respectively in order to have maximum isolation in X-band. The dimensions used in designing have been given in Table 1.

2.1 Switch working

The device operation states are shown in Fig. 2a, b. In state 1 with bridge in up position, switch is ON and shows insertion loss. OFF state can be achieved by pulling down the beam in the down position through electro-static actuation.

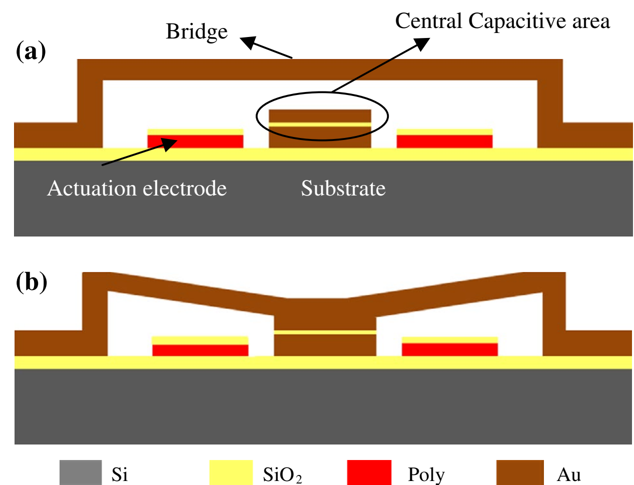

Fig. 2 Cross-sectional view for switch working

Figure 2b shows the isolation state when bridge provides the ground to the float central capacitive area.

3 Electrical response

RF response is the function of the ratio of up-state capacitance to the down-state capacitance and given by Eqs. (1–3):

$$C_{up} = \varepsilon_o A_{up}/d_o \tag{1}$$

$$C_{down} = \varepsilon_o \varepsilon_r A_{down}/t_{ox} \tag{2}$$

$$C_{ratio}(C_{down}/\ C_{up}) = \varepsilon_r A_{down} d_o/t_{ox} A_{up} \tag{3}$$

where, A_{up} = capacitive overlap area in up-state, A_{down} = capacitive overlap area in down-state, ε_r = relative permittivity, C_{up} = capacitance in the up-state of the switch, C_{down} = down-state capacitance of the switch and C_{ratio} = ratio of the capacitance in down-state to the up-state. A high capacitance ratio is desirable as more down capacitance provides good isolation and less capacitance in up-state provides good insertion loss. The capacitance in the up-state of the

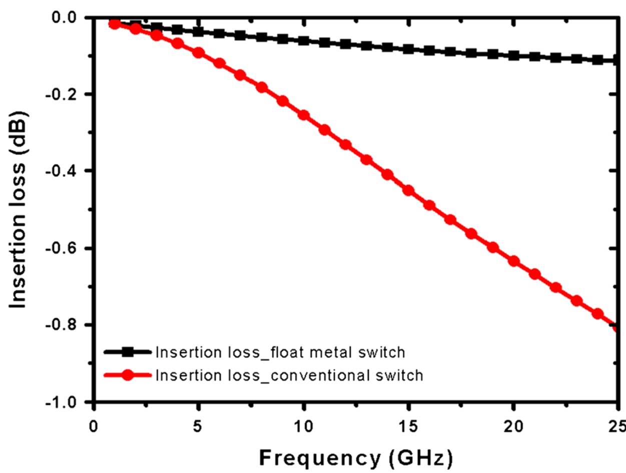

Fig. 3 Comparison of insertion loss of both switches

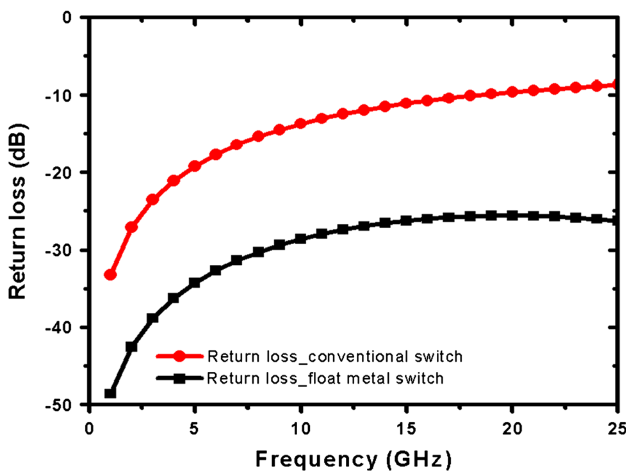

Fig. 4 Return loss of float metal vs. conventional switch

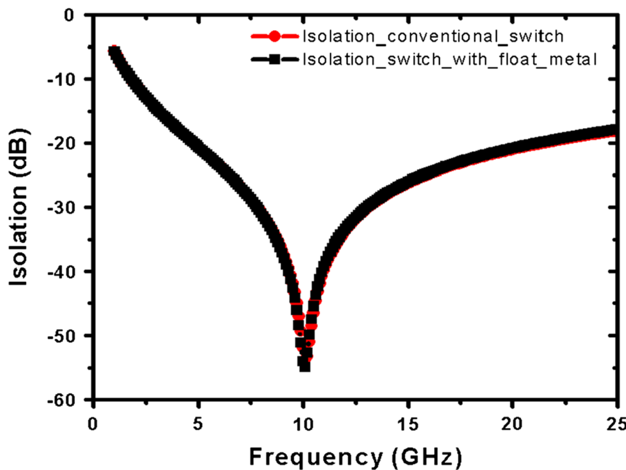

Fig. 5 Isolation of both devices

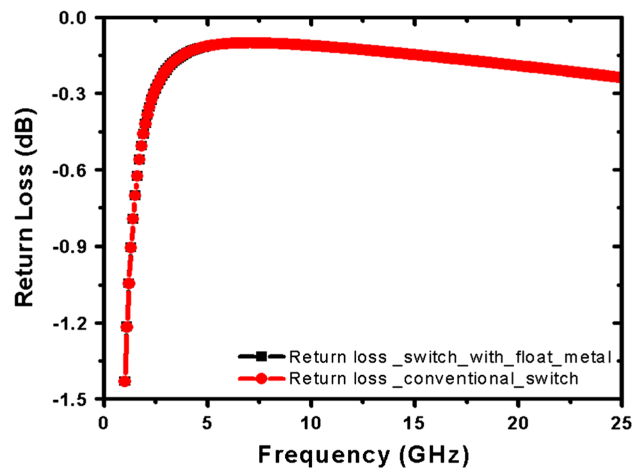

Fig. 6 Return loss of float metal vs. conventional switch in OFF state

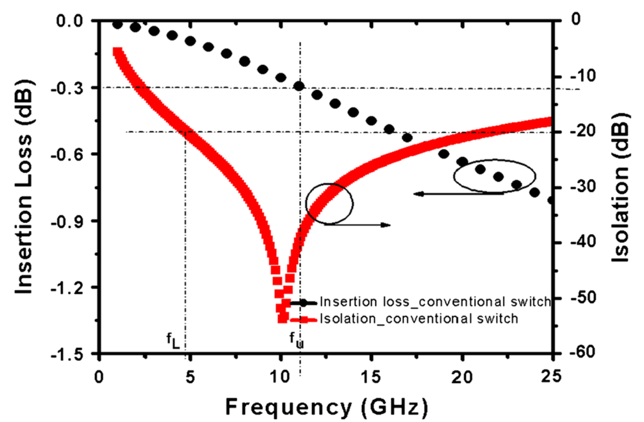

Fig. 7 Insertion loss and isolation characteristics of conventional switch

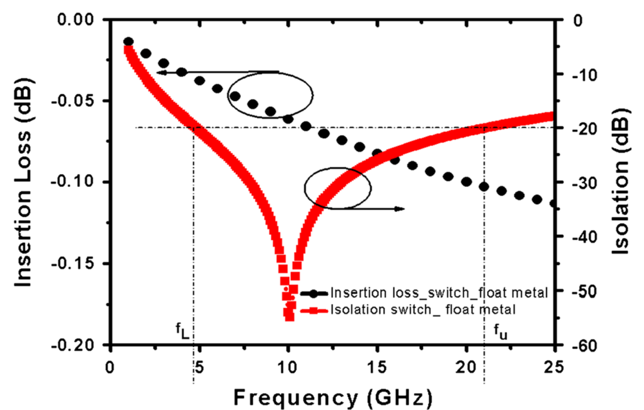

Fig. 8 Insertion loss and isolation characteristics of float metal switch

switch is reduced by utilizing the float metal concept. The device with float metal is having $A_{float_RF} = 90 \times 50\,\mu m^2$ whereas conventional $A_{con_RF} = 310 \times 90\,\mu m^2$.

$$C_{up_float} = \varepsilon_o 90 \times 50/d_o \quad (4)$$

$$C_{up_Con} = \varepsilon_o 310 \times 90/d_o \quad (5)$$

$$C_{up_float}/C_{up_Con} \approx 1/6 \quad (6)$$

Thus, from Eq. 6 C_{up_float} is around 6 times less than the C_{up_Con}. In order to determine the RF response electromagnetic simulation has been done through Ansys HFSS™. Insertion losses for the both devices have been plotted in Fig. 3. Insertion loss of 0.01–0.11 dB and 0.02–0.81 dB has been observed in case of float metal and conventional switch respectively in the frequency range from 1 to 25 GHz.

Return loss is also improved from 33.27–8.67 dB to 48.65–26.27 dB over the frequency range 1–25 GHz as shown in Fig. 4. In the OFF state both devices have same isolation and return loss characteristics as shown in Figs. 5, 6, respectively. This has happened as both devices have same inductance and capacitance in the down-state.

3.1 Switches bandwidth

The switch bandwidth can be calculated from the lower and the upper operating frequency.

Lower frequency (F_L) is limited by the minimum isolation, whereas the upper frequency (f_u) either by maximum insertion or minimum isolation. For bandwidth calculation an acceptable maximum insertion loss of 0.3 dB and minimum isolation of 20 dB has been chosen. It is observed from Fig. 7 that upper operating frequency is limited by insertion loss. Switch has $f_L = 4.8$ GHz and $f_u = 11$ GHz. This results in a bandwidth of 6.2 GHz in conventional design. The switch with float metal has $f_L = 4.8$ GHz and $f_u = 21$ GHz and a bandwidth of 16.2 GHz as shown in Fig. 8. In case of float metal switch maximum insertion loss limit can be changed down to 0.1 dB without affecting the bandwidth.

3.2 Self actuation and stiction due to RF power

The shunt capacitive RF-MEMS switch can handle certain power in the ON and OFF state. If the input power is sufficient to provide a voltage higher or equal to pull-in voltage of the device through the central overlap area, then under this condition self actuation of switch will occur without any d.c bias voltage. The input power corresponding to self actuation can be determined from Eqs. (7–10) as follows:

$$P_{in} = V_{RF}^2/Z_0 \quad (7)$$

$$P_{in} = V_{eq}^2/Z_0 \quad (8)$$

$$P_{S1}(V_{p1cpw}^2/Z_0) = 2.67\ \text{W} \quad (9)$$

$$P_{S2}(V_{p2cpw}^2/Z_0) = 0.63\ \text{W} \quad (10)$$

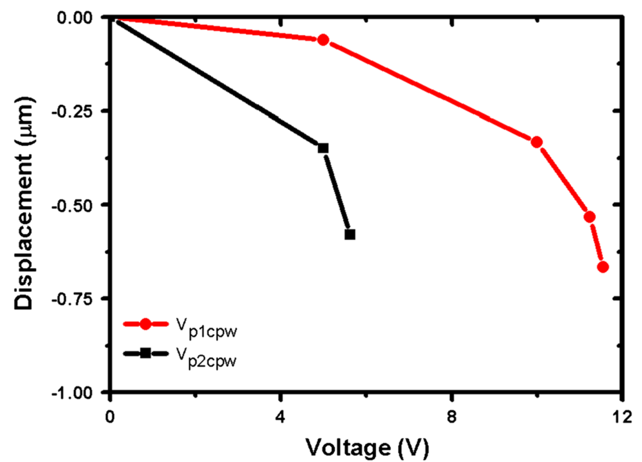

Fig. 9 Pull-in voltage under central overlap area for both switches

where P_{in} = input power, P_{S1}, P_{S2} = self actuation power in float metal and conventional design respectively, Z_0 (characteristic impedance of the line) = 50 Ω, V_{RF} = r.m.s value of the RF signal, V_{eq} = equivalent d.c voltage, V_{p1cpw} (Pull-in voltage due to central overlap area in float metal switch) = 11.56 V and V_{p2cpw} (Pull-in voltage due to central overlap area in conventional switch) = 5.6 V. FEM based simulation has been done through coventorware® to determine the pull-in voltage as shown in Fig. 9. It can be seen that the float metal device can handle around four times more input power without self actuation.

In down-state, stiction can occur if RF power is sufficient to provide a pull-down force which is higher or equal to the spring restoring force. The power needed to hold the switch in down-state can be obtained from Eqs. (11, 12) (Peroulis et al. 2004). The hold down power is dependent on frequency unlike the self actuation power. Thus, lower and higher frequencies have been taken from switches bandwidth for obtaining the hold down power.

$$P_{h1} = 27A_{electro}V_{p1}^2 t_{ox}^2[1 + 9.28f^2C_{down}^2Z_0^2]/8g_0A_{float_RF}Z_0 = 10.88 \text{ to } 204.88\ \text{W} \quad (11)$$

$$P_{h2} = 27A_{electro}V_{p2}^2 t_{ox}^2[1 + 9.28f^2C_{down}^2Z_0^2]/8g_0A_{con_RF}Z_0 = 2.06 \text{ to } 10.70\ \text{W} \quad (12)$$

where, P_{h1}, P_{h2} = hold down the power for float metal and conventional design respectively, and $V_{p1,2}$ (11.75 V, 12.75 V) pull-in voltage of the float metal switch and conventional switch respectively as shown in Fig. 10. For proper functionality of switch power input must be less than the minimum of self actuation power and hold down power. It is found that input power should be less than 0.63 W for the conventional switch and 2.67 W for the float

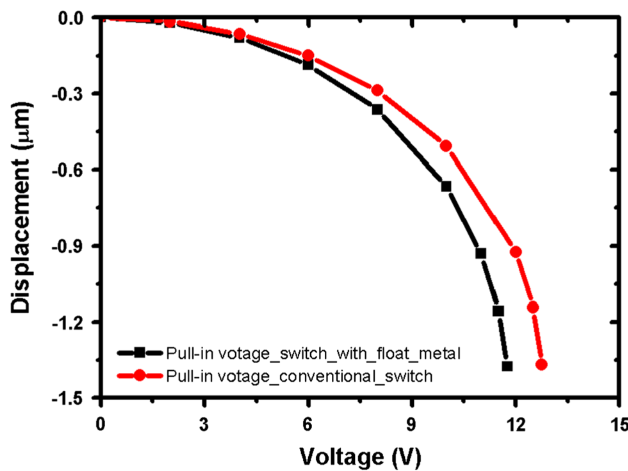

Fig. 10 Pull-in voltage of the float metal vs. conventional switch

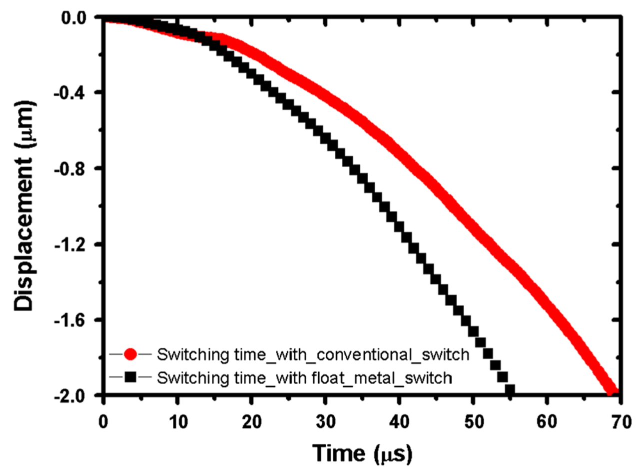

Fig. 11 Switching time response of both switches

metal design. The power input is increased around four times in the float metal device.

Another reason for stiction in down-state could be due to the electrostatic force, capillary force, hydrogen bonding, and Van der Waal forces. Float metal switch alleviates this problem as well, due to a reduction in the magnitude of the section forces (Tas et al. 1996; Bansal et al. 2013) caused by central capacitive overlap area compared to the conventional device.

4 Electro-mechanical and dynamic response

In electro-mechanical response pull-in voltage is the parameter of concern. Pull-in voltage is dependent on the length, width, thickness of flexure, Young's modulus, initial gap between electrode and movable structures and actuation area. Pull-in voltage of 12.75 and 11.75 V has been obtained through FEM simulation in case of conventional and float metal switch respectively as shown in Fig. 10.

In dynamic response the switching speed of MEMS switch is of main interest for many telecommunication applications. The switching time depends on various mechanical and electrical parameters like natural frequency of the movable parts, damping and ratio of pull-in to applied voltage. FEM simulated switching time has been given in Fig. 11. Float metal switch has less switching time as compared to conventional design due to decrease in mass through reduced central overlap area.

5 Conclusion

The switch with the conventional approach and using the float metal concept has been designed and investigated. The considerable improvement in insertion loss has been seen as compared to the conventional switch. OFF state response is same in both the devices because of same inductance and capacitance in the down-state. In float metal switch bandwidth is increased around 2.5 times than that of conventional switch. Input power is increased around 4 times without self bias and hold down problem. The pull-in voltage and switching time have also been reduced from 12.75 V to 11.75 V and 69.62 μs to 56.41 μs. The designed device can be useful for the multi-band applications.

References

Angira M, Sundaram GM, Rangra KJ, Bansal D, Kaur M (2013) On the investigation of an interdigitated, high capacitance ratio shunt RF-MEMS switch for X-band applications. In: Proceeding of NSTI Nanotech, Washington, DC, vol 2, pp 189–192

Armenta CJA, Porter S, Marvin A (2012) Reconfigurable Phased Array Antennas with RF-MEMS on a PCB Substrate. In: Proceeding of Antennas and Propagation, Loughborough, pp 1–5

Bansal D, Kumar A, Sharma A, Kumar P, Rangra KJ (2013) Design of novel compact anti-stiction and low insertion loss RF-MEMS switch. J Microsyst Technol. doi:10.1007/s00542-013-1812-1S

Brown ER (1998) RF-MEMS Switches for reconfigurable integrated circuits.IEEE Trans Microw Theory Tech 46:1868–1880

Dey S, Koul SK (2012) Design and development of a surface micro-machined push–pull-type true-time-delay phase shifter on an alumina substrate for Ka-band T/R module application. J Micromech Microeng 22:125006–1250026

DiNardo S, Farinelli P, Giacomozzi F, Mannocchi G, Marcelli R, Margesin B, Mezzanotte P Mulloni, V Russer, Sorrentino R, Vitulli F, Vietzorreck L (2006) Broadband RF-MEMS Based SPDT. In: Proceeding of European Microwave Conference, Manchester, pp 1727–1730

Entesari K, Rebeiz GM (2005) Differential 4-bit 6.5–10 GHz RF-MEMS tunable filter. IEEE Trans Microw Theory Tech 53:1103–1110

Fomani AA, Mansour RR (2009) Miniature RF-MEMS switch matrices. In: Proceeding of IEEE MTT-S Microwave Symposium Digest, Boston, pp 1221–1224

Giacomozzi F, Calaza C, Colpo S, Mulloni V, Collini A, Margesini B, Farinelli P, Casini F, Marcelli R, Mannocchi G, Vietzorreck L (2008) Development of high con coff ratio RF-MEMS shunt switches. Roman J Inf Sci Tech 11:143–151

Guo XL, Jin Y (2011) Miniature and tunable millimeter-wave low-pass filter with MEMS switch. J Solid-State Electron, Elsevier 63:145–148

Kang S, Kim HC, Chun K (2009) A low-loss, single-pole, four-throw RF-MEMS switch driven by a double stop comb drive. J Micromech Microeng 19:035011–035021

Peroulis D, Pacheco S, Sarabandi M, Katehi Linda PB (2000) MEMS devices for high isolation switching and tunable filtering. In: Proceeding of IEEE MTT-S Microwave Symposium Digest, Boston, pp 1217–1220

Peroulis D, Pacheco S, Katehi LPB (2004) RF-MEMS switches with enhanced power-handling capabilities. IEEE Trans Microw Theory Tech 52:59–68

Rangra K (2005) Electrostatic Low Actuation Voltage RF-MEMS Switches for Telecommunications, Ph.D. Thesis, Department of Information Technology, University of Trento, Trento, Italy

Rangra K, Margesin B, Lorenzelli L, Giacomozzi F, Collinni C, Zen M, Gsonicini S, Tin LD, Gaddi R (2005) Symmetric toggle switch—a new type of RF-MEMS switch for telecommunication applications: design and fabrication. Sens Actuators A 123:505–514

Razeghi A, Ganji BA (2013) A novel design of RF-MEMS dual band phase shifter. J Microsyst Technol. doi:10.1007/s00542-013-1921-x

Rebeiz GM (2003) RF-MEMS theory, design and technology, 2nd edn. Wiley, New Jersey

Rebeiz GM, Tan GL, Hayden JS (2002) RF-MEMS phase shifters: design and applications. IEEE Microwave Magazine 3(2):72–81

Rebriz GM, Muldavin JB (2001) RF-MEMS switches and switch circuits. IEEE Microw Mag 2(4):59–71

Tas N, Sonnenberg T, Jansen H, Legtenberg R, Elwenspoek M (1996) Stiction in surface micromachining. J Micromech Microeng 6:385–397

Tilmans HAC, Raedt WD, Beyne E (2003) MEMS for Wireless communications from RF-MEMS components to RF-MEMS SiP. J Micromech Microeng 13:139–163

Yua AB, Liua AQ, Zhang QX, Alphonesa A, Zhua L, Shacklockc AP (2005) Improvement of isolation for MEMS capacitive switch via membrane planarization. Sens Actuators A 119:206–213

Yua AB, Liua AQ, Zhang QX, Yu AB, Hosseini HM (2006) Effects of surface roughness on electromagnetic characteristics of capacitive switches. J Micromech Microeng 16:2157–2166